



HAL
open science

Contrasting response strategies of sulfate-reducing bacteria in a microbial consortium to As^{3+} stress under anaerobic and aerobic environments

Miaomiao Li, Jun Yao, Yating Wang, Geoffrey Sunahara, Robert Duran, Jianli Liu, Bang Liu, Houquan Liu, Bo Ma, Hao Li, et al.

► To cite this version:

Miaomiao Li, Jun Yao, Yating Wang, Geoffrey Sunahara, Robert Duran, et al.. Contrasting response strategies of sulfate-reducing bacteria in a microbial consortium to As^{3+} stress under anaerobic and aerobic environments. *Journal of Hazardous Materials*, 2024, 465, pp.133052. 10.1016/j.jhazmat.2023.133052 . hal-04355228

HAL Id: hal-04355228

<https://univ-pau.hal.science/hal-04355228>

Submitted on 25 Mar 2024

HAL is a multi-disciplinary open access archive for the deposit and dissemination of scientific research documents, whether they are published or not. The documents may come from teaching and research institutions in France or abroad, or from public or private research centers.

L'archive ouverte pluridisciplinaire **HAL**, est destinée au dépôt et à la diffusion de documents scientifiques de niveau recherche, publiés ou non, émanant des établissements d'enseignement et de recherche français ou étrangers, des laboratoires publics ou privés.

1 Contrasting response strategies of sulfate-reducing bacteria in a microbial
2 consortium to As³⁺ stress under anaerobic and aerobic environments

3
4
5 Miaomiao Li¹, Jun Yao^{1,*}, Yating Wang¹, Geoffrey Sunahara^{1,2}, Robert Duran³, Jianli Liu¹,
6 Bang Liu^{1,3}, Houquan Liu¹, Bo Ma¹, Hao Li¹, Wancheng Pang¹, Ying Cao¹

7
8
9 ¹ Research Center of Environmental Science and Engineering, China University of Geosciences
10 (Beijing), 29 Xueyuan Road, Haidian District, Beijing 100083, China

11 ² Department of Natural Resource Sciences, McGill University, 21111 Lakeshore Drive,
12 Ste-Anne-de-Bellevue, Quebec, H9X 3V9, Canada

13 ³ Université de Pau et des Pays de l'Adour, UPPA/E2S, IPREM CNRS 5254, Pau, France

14
15
16 * Corresponding author:

17 Jun Yao (E-mail: yaojun@cugb.edu.cn)

18 School of Water Resource and Environment, Research Center of Environmental Science and
19 Engineering, China University of Geosciences (Beijing), 29 Xueyuan Road, Haidian District,
20 100083, Beijing, China

23 **Abstract**

24 The sulfate-reducing efficiency of sulfate-reducing bacteria (SRB) is strongly influenced
25 by the presence of oxygen, but little is known about the oxygen tolerance mechanism of SRB
26 and the effect of oxygen on the metalliferous immobilization by SRB. The performance
27 evaluation, identification of bioprecipitates, and microbial and metabolic process analyses
28 were used here to investigate the As³⁺ immobilization mechanisms and survival strategies of
29 the SRB1 consortium under different oxygen-containing environments. Results indicated that
30 the sulfate reduction efficiency was significantly decreased under aerobic (47.37%) compared
31 with anaerobic conditions (66.72%). SEM analysis showed that under anaerobic and aerobic
32 conditions, the morphologies of mineral particles were different, whereas XRD and XPS
33 analyses showed that the most of As³⁺ bioprecipitates under both conditions were arsenic
34 minerals such as AsS and As₄S₄. The abundances of *Clostridium_sensu_stricto_1*,
35 *Desulfovibrio*, and *Thiomonas* anaerobic bacteria were significantly higher under anaerobic
36 than aerobic conditions, whereas the aerobic *Pseudomonas* showed an opposite trend.
37 Network analysis revealed that *Desulfovibrio* was positively correlated with *Pseudomonas*.
38 Metabolic process analysis confirmed that under aerobic conditions the SRB1 consortium
39 generated additional extracellular polymeric substances (rich in functionalities such as Fe-O,
40 S=O, C=O, and -OH) and the anti-oxidative enzyme superoxide dismutase to resist As³⁺
41 stress and oxygen toxicity. New insights are provided here into the oxygen tolerance and
42 detoxification mechanism of SRB and provide a basis for the future remediation of heavy
43 metal(loid)-contaminated environments.

44 **Keywords:** Sulfate-reducing bacteria, Response strategies, As³⁺, Anaerobic, Aerobic

45 **1. Introduction**

46 Heavy metal(loid) pollution of soil and industrial wastewater (including acid mine
47 drainage) is a global environmental concern with the presence of more than 10 million
48 polluted sites worldwide (Fei et al., 2019; Xiao et al., 2019; Xu et al., 2021b). It is well
49 known that the cumulative effects of industrialization and anthropogenic activities have led to
50 severe pollution by heavy metal(loid)s (HMs) (Chun et al., 2021) caused by the construction
51 of mines, metal smelters, coal-fired power stations, and manufacturing factories (Yun et al.,
52 2018; Zhang et al., 2021; Li et al., 2022a; Li et al., 2022b). Superfluous HMs entering into
53 the environment can severely diminish soil and water quality and productivity, thereby
54 disturbing the balance of the surrounding ecosystem, and decreasing the stability of the
55 microbial community (Chun et al., 2021; Ran et al., 2021; Zhang et al., 2021). The release of
56 HMs into the environment can also pose a serious health threat to humans and sensitive
57 species of the food web (Ran et al., 2021; Li et al., 2015; Liu et al., 2017). Therefore, it is
58 important to adopt appropriate remediation strategies for HM pollution.

59 Microbial strategies offer a viable and eco-friendly alternative to the stabilization of
60 HMs using organisms such as fungi, bacteria, and plants (Sun et al., 2017; Chun et al., 2021).
61 Biological treatment based on sulfate-reducing bacteria (SRB) is an increasingly attractive
62 remediation strategy due to its cost-effectiveness, and ability to remove and immobilize HMs
63 (Liu et al., 2018; Bao et al., 2020; Dev et al., 2021; Si et al., 2023). SRB is generally regarded
64 as strict anaerobic bacteria that are widely distributed in seawater, marine sediments, hot
65 springs, and geothermal fields, as well as in oil and gas wells (Cypionka et al., 1985;
66 Ravenschlag et al., 2000; de Matos et al., 2018) and acid mine drainage (Giloteaux et al.,

2013), where they play an important role in the global S-cycle (Zhou and Xing, 2021; Si et al., 2023). SRB can use sulfate (SO_4^{2-}) as the terminal electron acceptor to generate sulfide (S^{2-}), which reacts with free HM ions to form insoluble metal sulfide precipitates (Liu et al., 2018; Lv et al., 2022). The role of the biomineralization process has been studied in recent years (Gu et al., 2021; Zampieri et al., 2021; Yan et al., 2023). For example, *Desulfovibrio desulfuricans* can remove Zn as zinc sulfide (ZnS) in the presence of SO_4^{2-} from acid mine drainage (Hwang and Jho, 2018). Whereas an enriched SRB consortium achieved the simultaneous removal of multiple metals, including Cr, Cu, Ni, and Zn (Kieu et al., 2011). SRB can also enhance the passivation performance of biochar for immobilizing HMs (Si et al., 2023). During the application of SRB for HMs remediation, the availability of an anaerobic environment is not often assured, and SRB will face exposure to an oxygenated environment as it transits down the soil column. From the initial aerobic layer, and the SRB gradually penetrates down to the anoxic layer interface and finally reaches the anaerobic layer interface at a certain depth. Therefore, for practical purposes, the survival of SRB in oxygen-containing environments must be elaborated. To the best of our knowledge, most peer-reviewed SRB studies have been conducted in anaerobic environments. The immobilization of HMs by SRB under aerobic conditions has rarely been reported. Therefore, this knowledge gap regarding the effect of oxygen on the metalliferous immobilization by SRB should be investigated.

The fermentation efficiency of an anaerobic system could be facilitated by a small amount of oxygen (Nguyen et al., 2019), which enhances the diversity and activity of facultative bacteria to maintain the activity of oxygen-sensitive anaerobic bacteria. The

89 presence of oxygen may create a niche for specific bacteria in an anaerobic consortium to
90 facilitate biological metabolic processes, such as the methanogen and organohalide-respiring
91 bacteria (Chen et al., 2023). Furthermore, the oxygen tolerance of anaerobic bacteria could be
92 due to the consumption of oxygen by co-existing aerobic bacteria or that aerobic bacteria
93 protect anaerobic bacteria from oxygen exposure (Dalsgaard et al., 2014; Oshiki et al., 2016;
94 Yue et al., 2018; Okabe et al., 2023). These studies indicate that anaerobic bacteria can
95 survive under aerobic conditions and possess oxygen tolerance, thereby providing support for
96 the aerobic survival of SRB (Fourçans et al., 2007). However, relatively little is known about
97 the survival strategies of SRB in oxygen-containing environments.

98 The sulfate-reducing consortium, SRB1, which was obtained in a previous study (Li et
99 al., 2022b), can still immobilize As^{3+} and retain sulfate-reducing function in the tailings
100 remediation process (under aerobic conditions), and suggests that SRB1 can tolerate a certain
101 concentration of oxygen. Therefore, the objectives of the present study are (1) to compare the
102 differences in the immobilization mechanism of As^{3+} by an SRB1 consortium under
103 anaerobic and aerobic conditions and (2) to reveal the survival strategies of SRB in the SRB1
104 consortium under oxygen-containing conditions from a molecular perspective.

105 **2. Materials and methods**

106 2.1 Chemicals, reagents, and culture media

107 Analytical grade sodium arsenite ($NaAsO_2$, CAS 7784-46-5) was purchased from
108 Beijing Inokay Technology (China). The standard reference material GSB 04-1767-2004
109 (obtained from the National Center of Analysis and Testing for Nonferrous Metals and

110 Electronic Materials, China) confirmed the analytical quality of arsenic determinations.
111 Information on medium A is detailed in Supplementary Text S1. All other chemicals used in
112 this study were obtained from commercial sources and were at least of analytical grade
113 purity.

114 2.2 Biosystem setup and operational conditions

115 The SRB1 microbial consortium was obtained from Huilong nonferrous metal smelter
116 soil, which was heavily contaminated with arsenic (Li et al., 2022b). The SRB1 microbial
117 consortium was cultured in medium A. Batch experiments were performed by adding
118 NaAsO₂ stock solution (2000 mg/L) to medium A to achieve an initial concentration of 50 mg
119 As³⁺ /L. This concentration was selected because the SRB1 consortium can function well at
120 50 mg As³⁺ /L (Li et al., 2022b).

121 All batch experiments were performed using 250 mL serum bottles filled with
122 approximately 200 mL medium A and sterilized by autoclaving at 121°C for 25 min and
123 protected against light by aluminum foil to minimize photo-oxidation of As³⁺. The
124 experimental group (nine serum bottles) was inoculated with SRB1 microbial consortium and
125 was treated under anaerobic, anoxic, and aerobic conditions, whereas the abiotic controls
126 (nine serum bottles) received the same treatments but did not contain added inoculum. The
127 anaerobic experiments were degassed using bubbled pure N₂ for 10 min and sealed with
128 rubber plugs. The anoxic experiments were sealed using an airtight cap, and the aerobic
129 experiments were sealed with an air-porous membrane. The initial dissolved oxygen (DO)
130 concentrations under three conditions were measured by a DO meter (PreSens Fibox 4 trace,
131 Germany). Sample aliquots were taken daily, and the biomass and solid samples were taken

132 and harvested by centrifugation at 8000 rpm for 10 min at specific time points (0, 2, 5, and 7
133 d) under anaerobic, anoxic, and aerobic conditions for the microbial and mineralogical
134 analyses. All treatments were performed in triplicate and incubated at 30°C for 7 d.

135 2.3 Immobilization of As³⁺ studies

136 2.3.1 Aqueous speciation analysis

137 The microbial culture sample was centrifuged and then the supernatant was passed
138 through a 0.22- μ m filter to facilitate subsequent analysis. The pH, ORP, biomass of bacterial
139 culture (OD₆₀₀), and the concentrations of total As, SO₄²⁻, and S²⁻ were determined in the
140 samples (details in Supplementary Text S2).

141 2.3.2 Solid phase analysis

142 The samples collected under the studied conditions during specific periods were
143 centrifuged before being washed with ultrapure water and freeze-dried for 24 h. These
144 samples were sent to Beijing Weizhen Technology (China) for further analysis. Detailed
145 information is provided in Supplementary Text S2.

146 2.4 Microbial analysis

147 The analyses of microbial communities of the collected SRB1 consortium exposed to 50
148 mg As³⁺/L were carried out at 0, 2, 5, and 7 d under anaerobic, anoxic, and aerobic culture
149 conditions. The details of total genomic DNA extraction are described in Supplementary Text
150 S3. The raw sequence data of the bacterial community obtained in this study was submitted to
151 the NCBI database (Accession No. PRJNA983256). The microbial extracellular polymeric
152 substances (EPS) consisting of extracellular protein (PN), polysaccharide (PS), and

153 humic-like substances (HS) were also determined and quantified at 2, 5, and 7 d under the
154 studied incubation conditions. Moreover, it is generally accepted that reactive oxygen species
155 (ROS) can be produced after molecular oxygen enters the cells. Being potent oxidants ROS
156 can damage DNA and proteins (Morris, 1975; Okabe et al., 2023). Microorganisms can
157 secrete anti-oxidative enzymes to detoxify ROS and adapt to excess oxygen (Jenney et al.,
158 1999). Catalase (CAT), superoxide dismutase (SOD), and peroxidase (POD) activities were
159 determined at day 7, according to Okabe et al (2023), as described in Supplementary Text S4.

160 2.5 Statistical analysis

161 The relative abundance, heatmap, and co-occurrence patterns were plotted using
162 commercial software (as described in Supplementary Text S5). Spearman's correlation
163 coefficient analysis ($R > |0.7|$ and $P < 0.05$) was calculated to confirm the biological
164 interactions. Statistically significant differences between different groups at $P < 0.05$ were
165 carried out by the one-way analysis of variance (ANOVA) using SPSS software (ver.18.0).
166 Data was expressed as mean \pm SD (standard deviation) ($n = 3$).

167 3. Results and discussion

168 3.1 Performance of SRB1 consortium on As^{3+} immobilization

169 Using an initial As^{3+} concentration of 50 mg/L, the performance of the SRB1 consortium
170 was determined under anaerobic, anoxic, and aerobic conditions. There were significant
171 differences in DO under anaerobic, anoxic and aerobic conditions, which reached 3.05 ± 0.14
172 mg/L, 5.62 ± 0.21 mg/L and 6.35 ± 0.12 mg/L, respectively ($P < 0.05$, Fig. S1). The pH of
173 the SRB1 consortium decreased initially on day 1 (from pH 5.58-5.68 to pH 5.44-5.49) under

174 the three conditions, and then increased from day 2 to day 7 (Fig. 1A). There was no
175 difference in pH between anaerobic and anoxic conditions ($P > 0.05$), and the pH increased
176 slightly from pH 5.58-5.68 to ~ pH 6.0 on day 7. It was noteworthy that the pH increased by
177 35.71% from the initial pH 5.6 ± 0.1 to pH 7.6 ± 0.1 on day 7 ($P < 0.05$) under the aerobic
178 conditions, which was higher than those under anaerobic or anoxic conditions. This increase
179 in pH was likely attributed to HCO_3^- (in the system) that consumes H^+ to increase the pH
180 (Liu et al., 2018). In contrast, the pH of the control group remained stable at approximately
181 pH 4.5.

182 There were significant differences among the ORP variation of the SRB1 consortium (P
183 < 0.05) under the three conditions (Fig.1A). The initial ORP was maintained below zero,
184 likely due to the initial addition of the inoculated microbial consortium. The ORP varied
185 similarly under the anaerobic and anoxic conditions ($P > 0.05$), decreasing slowly from day 1
186 (-20 ± 14.7 mV) to day 7 (-8 ± 10.7 mV). Under aerobic conditions, the ORP decreased
187 sharply from day 1 to day 2, and subsequently remained stable, from an initial value of $-38 \pm$
188 10 mV and reached about -127 ± 8.7 mV on day 7. The pH and ORP are important
189 environmental factors for the function of microorganisms (Jin and Kirk, 2018). The present
190 results indicate that the pH and ORP under aerobic conditions were different compared to
191 those under anaerobic and anoxic conditions and suggest that aerobic conditions provide a
192 favorable habitat for SRB1.

193 The density of plankton biomass (at OD_{600}) under the different culture conditions is
194 shown in Fig. 1B. Under anaerobic conditions, the plankton biomass gradually increased and
195 reached 2.4 ± 0.1 on day 7. Under anoxic conditions, the plankton biomass increased slowly

196 from day 0 to day 4, entered a plateau period, and then began to decline after day 5, reaching
197 an OD₆₀₀ of 1.4 ± 0.1 on day 7. Under aerobic conditions, the plankton biomass increased
198 sharply from the initial OD₆₀₀ of 0.8 ± 0.1 to 3.2 ± 0.1 during 7 d of operation, which was
199 higher than that under anaerobic and anoxic conditions ($P < 0.05$), indicating that aerobic
200 conditions were more conducive to the growth of SRB1 microorganisms.

201 The decrease in the total As concentration in the aqueous phase was noticeable during
202 the first three days of the study (Fig. 1B). Under anaerobic conditions, the total As
203 concentration (mg/L) continued to decrease after day 3, from the initial value of 54.7 ± 1.1 to
204 6.5 ± 1.6 on day 7. Under anoxic conditions, the total As concentration decreased during the 4
205 d of incubation, from the initial 54.6 ± 1.2 to 9.1 ± 0.6 on day 4 and then increased to $10.1 \pm$
206 0.9 on day 7. Interestingly, the total As concentration gradually increased under aerobic
207 conditions from 11.1 ± 0.6 on day 3 to 21.1 ± 1.9 on day 7, which was higher than that under
208 anaerobic (6.5 ± 1.6) or anoxic conditions (10.1 ± 0.9) on day 7. This difference was probably
209 related to the oxidation of As-containing minerals in the aerobic water environment
210 suggesting that aerobic and anoxic conditions do not favor As³⁺ immobilization by SRB.

211 To investigate the performance of the SRB1 consortium on sulfate reduction under
212 anaerobic, anoxic, and aerobic conditions, the dynamic changes of SO₄²⁻ and S²⁻
213 concentrations were determined. The concentration of SO₄²⁻ (mg/L) decreased from the
214 initial 691.2 ± 4.3 and 722.3 ± 2.0 to 230.0 ± 10.1 and 406.5 ± 6.9 during the 7 d of operation
215 ($P < 0.05$), under anaerobic and aerobic conditions, respectively (Fig. 1C). However, the
216 SO₄²⁻ concentration decreased narrowly under anoxic conditions, and the SO₄²⁻ reduction
217 efficiency was only 10.3% during operation. On the other hand, the production of S²⁻ under

218 anoxic conditions was much lower than that observed under either anaerobic or aerobic
219 conditions (Fig. 1C), which coincided with the dynamic changes of SO_4^{2-} . The dynamic
220 changes of biomass and total As concentration, along with the reduction of SO_4^{2-} and the
221 production of S^{2-} imply that the behavior of the SRB consortium under aerobic conditions
222 differs compared to under anaerobic conditions. This observation suggests that the growth of
223 SRB1 microorganisms is favored under aerobic conditions which is in contrast to the
224 immobilization of As^{3+} and the reduction of SO_4^{2-} that are favored under anaerobic
225 conditions.

226 3.2 Identification of bioprecipitates under varied conditions

227 The SEM, XRD, and XPS analyses were used to investigate the transformation process
228 of SRB1 consortium solid phase morphology for different durations under the three studied
229 conditions. In SEM images (Fig. 2), the morphology of mineral particles was similar on day 2,
230 exhibiting multiple columnar clusters irrespective of the incubation condition. However, after
231 day 5, these mineral particles displayed an inconsistent appearance between the anaerobic
232 and aerobic conditions. Under anaerobic conditions, the solids took a smooth blanket-like
233 structure on day 5, despite the presence of nano-sized particles on the surface; transformation
234 into tight columnar clusters was seen on day 7. Compared to anaerobic conditions, many
235 nano-sized surficial particle layers were more dispersed and distributed from days 5 to 7
236 under aerobic conditions. The morphology of the solid phase under anoxic conditions was
237 similar to those found in the middle of aerobic and anaerobic exposures, with many
238 aggregates forming by day 5, and then converted to a porous flake-like cluster on day 7.

239 The XRD analysis showed that the main components of bioprecipitates were similar

240 under anaerobic and aerobic conditions (Fig. 3). During incubation, the indicative diffraction
241 peaks of AsS and As₄S₄ were detected, and the sharp peaks appeared at $2\theta = 13.231^\circ$ on day 7,
242 which indicates the presence of arsenolamprite (As). Uniquely, the ferrisymplesite
243 ($\text{Fe}_3(\text{AsO}_4)_2 \cdot 6\text{H}_2\text{O}$) appeared on day 7 under aerobic conditions. Thus, the XRD patterns
244 suggest that the main formation of bioprecipitates was weakly associated with anaerobic and
245 aerobic conditions during the short term and that aerobic conditions did not affect the
246 sulfate-reducing activity of the SRB1 consortium.

247 Further investigations using XPS analysis were performed to infer the formation and
248 composition of bioprecipitates, with a focus on determining the chemical species of As, Fe,
249 and S. The XPS spectrum related to As-3d was mainly divided into three particular peaks (eV)
250 at 41.28, 42.96, and 44.78, which were assigned to As(-I)-S, As(III)-S, and As(III)-O,
251 respectively. On day 7, the As-3d was similar under anaerobic and anoxic conditions (Fig. 4),
252 existing mainly as As(III)-S and As(III)-O. The additional As(-I)-S components were detected
253 in aerobic conditions only. Such observation suggested that the surficial arsenic-containing
254 sulfide minerals were oxidized before day 7 (Fig. 1B), consistent with the previous studies
255 (Feng et al., 2021; Chen et al., 2022).

256 The S 2p signals in XPS spectra contained mainly five peaks (eV) at approximately
257 163.08, 164.68, 168.69, and 170.28, corresponding to S_2^{2-} , S^0 , SO_4^{2-} , and $\text{S}_2\text{O}_3^{2-}$, respectively.
258 The S_2^{2-} had a higher content (%) under aerobic conditions (66.23) than under anaerobic
259 (54.35) and anoxic (24.74) conditions. Correspondingly, the SO_4^{2-} had a lower content under
260 the aerobic (11.92) than under the anaerobic (33.69) or anoxic (52.63) conditions. These
261 results suggested that the biological reduction of SO_4^{2-} under anoxic conditions was much

262 slower than that under the anaerobic and aerobic conditions, which coincided with the
263 previous changes of SO_4^{2-} concentration (Fig. 1C). Moreover, many intermediate-valent S
264 products were detected in the process of SO_4^{2-} reduction, such as $\text{S}_2\text{O}_3^{2-}$, S^0 , and SO_3^{2-} (Fig.
265 4).

266 The XPS spectra of Fe 2p were also analyzed and fitted with many peaks (eV), including
267 Fe^{2+} signals at 710.92 and 725.18, Fe^0 signals at 719.28 and 720.68, and different Fe^{3+}
268 signals at 712.88, 715.98, 717.08, 726.68, 728.58, and 729.48. Fe^{2+} is the chemical state of
269 Fe-oxide and sulfide species, and Fe^{3+} is the oxidized state (Xu and Fu, 2022). Under aerobic
270 and anoxic conditions, the integrated peak area of Fe^{3+} was higher than that under anaerobic
271 conditions, indicating that the iron oxidation was more intense under aerobic and anoxic
272 conditions. Therefore, although there are differences in the changes of As, Fe, and S species
273 under anaerobic and aerobic conditions, the SRB1 consortium can generally achieve sulfate
274 reduction and immobilize As in the form of arsenic minerals (AsS and As_4S_4) under anaerobic
275 and aerobic conditions. Moreover, Fe likely plays an important role in the process of As
276 detoxification.

277 3.3 Dynamics of microbial community structure

278 The microbial diversity of the SRB1 consortium incubated under the three studied
279 conditions was characterized through the 16S rRNA gene sequencing to identify the
280 interactions between microorganisms in samples taken at days 0, 2, 5, and 7. After
281 de-multiplexing and removing chimeras, a total of 936,663 valid reads were obtained from 12
282 samples of the SRB1 consortium, which were clustered into 410 operational taxonomic units
283 (OTUs) according to the sequence similarity of 97%. The sequencing coverage of all samples

284 was > 0.99, indicating that the constructed reads library was sufficiently reliable for further
285 analysis. Regardless of the conditions, the OTUs and Chao1 values gradually declined in the
286 first five days and increased subsequently (Table S1). The Shannon index significantly
287 increased after two days compared with the initial value, whereas the opposite trend was
288 observed in the Simpson index. These results showed that under arsenic stress, the microbial
289 community richness and diversity of the SRB1 consortium displayed a significant difference
290 during the experiment.

291 The microbial population structure of the SRB1 consortium under the three studied
292 conditions at the phylum level was altered significantly during sulfate reduction (Fig. S2).
293 Pseudomonadota is predominant in the initial community of the SRB1 consortium with a
294 relative proportion > 90.0%, decreased subsequently throughout the prolonged incubation in
295 all three conditions. In contrast, Bacillota was enriched after two days, and the relative
296 proportions (%) of Bacillota under anaerobic (43.8 - 45.0) and anoxic conditions (41.7 - 49.4)
297 were higher than that obtained under aerobic conditions (15.4 - 37.4) ($P < 0.05$). Bacteroidota
298 was also slightly enriched after five days, with the relative proportions of 5.6 -7.7 (anaerobic)
299 and 5.2 -6.4 (aerobic), respectively, whereas no obvious difference was seen under anoxic
300 conditions.

301 The top 15 predominant genera were identified (Fig. 5A). The taxa affiliated with
302 *unclassified_f_Enterobacteriaceae*, *Clostridium_sensu_stricto_1*, and *Pseudomonas* were the
303 most abundant genera, accounting for > 70% of the whole microbial sequences. The
304 microbial diversity and structures of the SRB1 consortium at the genus level were
305 significantly distinct under aerobic, anaerobic, and anoxic conditions (Fig. 5B). Compared to

306 the inoculum, the relative proportions of *Clostridium_sensu_stricto_1* and *Anaerocolumna*
307 showed a significant upward trend with the ongoing sulfate reduction. The relative
308 proportions (%) of *unclassified_f_Enterobacteriaceae* decreased greatly under anaerobic
309 (from 69.9 to 41.6), anoxic (from 67.3 to 40.6), and aerobic (74.5 to 16.0) conditions.

310 The relative proportions of the taxa affiliated with the anaerobic bacteria
311 *Clostridium_sensu_stricto_1*, *Anaerocolumna*, *Desulfovibrio*, and *Thiomonas* were higher
312 under anaerobic and anoxic conditions than under aerobic conditions ($P < 0.05$). In the
313 present study, the relative abundances (%) of *Clostridium_sensu_stricto_1* under anaerobic,
314 anoxic, and aerobic conditions were 31.0, 31.4, and 11.3, respectively.

315 *Clostridium_sensu_stricto_1* is affiliated with iron-reducing members and usually has high
316 relative abundances during changing redox conditions. *Anaerocolumna* was determined on
317 day 7 under aerobic conditions with an abundance of 0.4%, while its abundance under the
318 anaerobic and anoxic conditions reached 0.7% and 0.9%, respectively. *Anaerocolumna* (an
319 anaerobic bacteria) is widely found in the anaerobic digestive system and has a relatively
320 superior environmental resistance (Xu et al., 2021a). *Thiomonas* belongs to the facultative
321 chemolithoautotrophs and has a growth preference for a mixed nutrient medium containing
322 reducing inorganic S compounds and organic matter (Jia et al., 2022).

323 *Desulfovibrio*, a typical SRB widely present in anaerobic and anaerobic environments
324 (Zhou et al., 2014; Li et al., 2022c) was detected on day 5 under anaerobic, anoxic, and
325 aerobic conditions with an abundance (%) of 0.7, 0.9, and 0.2, respectively. In the present
326 study, the relative abundance of *Desulfovibrio* under aerobic conditions was significantly
327 lower than that under anaerobic or anoxic conditions. This implies that the abundance of

328 *Desulfovibrio* was positively and proportionally related to the oxygen concentration, which is
329 consistent with the normal survival law of anaerobic bacteria. Moreover, the presence of
330 *Desulfovibrio* under aerobic conditions also suggests that it can tolerate oxygen concentration
331 within a certain range.

332 The taxa affiliated with *Pseudomonas* showed an opposite trend, being detected on day 7
333 with a relative abundance (%) of 1.2, 13.2, and 57.4 under anaerobic, anoxic, and aerobic
334 conditions, respectively. Members of the *Pseudomonas* genera, gram-negative obligate
335 aerobe, can grow using different anaerobic mechanisms (Jia et al., 2022). For example,
336 *Pseudomonas* can change the hydrophobicity of its cell wall by adjusting the composition of
337 the cell membrane lipopolysaccharide, thus enhancing the interactions with other substances
338 (Rogers et al., 2020).

339 It is worth noting that the SRB1 bacteria can retain its sulfate-reducing activity under
340 aerobic conditions (Fig. 1C), indicating that sulfate-reducing bacteria (*Desulfovibrio*) can
341 survive and stay functional under aerobic conditions. Although SRBs are traditionally
342 considered strictly anaerobic, many studies have consistently observed aerobic survival and
343 oxygen resistance (Fournier et al., 2004; Ramel et al., 2013; Ramel et al., 2015; Chen and
344 Zhang, 2019). Certain SRB species can survive temporarily when exposed to oxygen
345 (Cypionka et al., 1985). *Desulfovibrio* is a relatively common class of SRB that plays a major
346 role in the S cycle (Chen and Zhang, 2019; Nagar et al., 2022). Risatti et al. (1994) analyzed
347 the microbial communities of cyanobacteria from saline-evaporated ponds and found that the
348 *Desulfovibrio* population was overwhelmingly dominant in oxygenated areas with light. In
349 addition, the co-culture experiments have shown that coexisting bacteria can consume oxygen

350 in the environment to aid *Desulfovibrio* survival in a high-oxygen environment (Sigalevich et
351 al., 2000; Vita et al., 2008). Therefore, the observation reported here is not only related to the
352 adaptation strategy of *Desulfovibrio* in an aerobic environment but also reflects the beneficial
353 contribution of co-existing bacteria (possibly the aerobes, e.g., *Pseudomonas*) in the SRB1
354 consortium, which would increase *Desulfovibrio* oxygen tolerance by consuming the oxygen
355 in the environment (Sigalevich et al., 2000; Chen and Zhang, 2019).

356 3.4 Co-occurrence patterns of bacterial communities and metabolic process variation

357 To further study the bacterial interactions in the SRB1 consortium, the microbial
358 co-occurrence patterns were constructed by the strong correlations (Spearman $R > |0.7|$) and
359 significant differences ($P < 0.05$) to filter the OTUs (Fig. 6A). The networks of the SRB1
360 consortium consisted of 206 nodes and 549 edges (Table S2). Pseudomonadota (34.95%) and
361 Bacillota (16.02%) affiliated phylotypes dominated the networks, followed by
362 Actinomycetota (11.17%), norank_k_Bacteria (10.68%), Acidobacteriota (8.25%),
363 Bacteroidota (7.77%), Gemmatimonadetes (3.4%), and Chloroflexi (1.94%).

364 Interestingly, 99% of edges were positively correlated, indicating that the
365 microorganisms in the SRB1 consortium could cooperate in response to arsenic and oxygen
366 stress. To investigate the hypothesis that symbiotic aerobic bacteria (*Pseudomonas*) in the
367 SRB1 consortium consume environmental oxygen to provide a niche for SRB (e.g.,
368 *Desulfovibrio*), the co-cultures were used to determine the species cooperation network at the
369 genus level (Fig. 6B). The screening condition was kept to only the genera whose sum of
370 relative abundance was $> 0.005\%$, and the filtered OTUs simultaneously appeared in five
371 samples. Spearman's correlation coefficient analysis ($R > |0.7|$ and $P < 0.05$) was then carried

372 out to investigate the interactions with each of the two genera (Li et al., 2023). These results
373 provide further evidence that the taxa affiliated with *Pseudomonas* had a positive cooperative
374 relationship with *Desulfovibrio* (Table S3). In future studies, pure strains of *Desulfovibrio* and
375 *Pseudomonas* genera should be screened from the SRB1 consortium, and the interactions of a
376 synthetic microbial community could be studied to further determine the survival strategy of
377 SRB under oxygen-containing conditions.

378 Moreover, extracellular polymeric substances (EPS) produced by SRB play an important
379 role in immobilizing HMs in the environment (Liu et al., 2021). Exposure to HMs could
380 induce microorganisms to generate EPS, forming complexes with metals as a defense
381 mechanism (Wang et al., 2014). The EPS includes proteins (PN), polysaccharides (PS),
382 humic substances (HS), and nucleic acids, among which proteins are a dominant component
383 affecting the fate of HMs (More et al., 2014; Yan et al., 2020). Therefore, the EPS fraction of
384 the SRB1 consortium was determined under anaerobic, anoxic, and aerobic conditions. Data
385 indicated that PN was the main EPS, followed by HS, and a small quantity of PS (Fig. 6C). It
386 is worth noting that these EPS components decreased progressively during incubation, which
387 was inseparable from the decrease in As concentrations because the production of EPS by
388 microorganisms was not needed for the As stress resistance (Wang et al., 2014). In addition,
389 the PN produced by the SRB1 consortium on day 2 under aerobic conditions was
390 significantly higher than under the other two conditions, which may be related to the response
391 of SRB to oxygen stress under aerobic conditions.

392 The FTIR analysis was used to determine the changes of functional groups on the EPS
393 fraction under the different incubation conditions (Zhao et al., 2023). No obvious shifts

394 occurred, as evidenced by the main absorption bands (cm^{-1}) (Fig. 6D) appearing at about 618
395 (Fe-O), 1108 (S=O), 1655 (C=O), and 3291 (-OH) in the FTIR spectrum of EPS (Barakan et
396 al., 2019; Feng et al., 2019; Zhang et al., 2019). Multifarious functional groups such as
397 -COOH, C-N, and C-H (Shi et al., 2020; Wang et al., 2021; Wu et al., 2023) were also
398 detected in the EPS. The -OH and -COOH were the key functional groups in the EPS of the
399 cell surfaces, which are relevant to PN and HS or PS (Wu et al., 2023), likely providing
400 potential binding sites for the exchange or complexation with As^{3+} (Zhao et al., 2023).

401 Additionally, the CAT, POD, and SOD activities of the SRB1 consortium were
402 determined under the three studied conditions on day 7 (Fig. S3). The results show that the
403 SRB1 consortium exhibited higher SOD activities (U/mL) under aerobic conditions (15.58)
404 than under anaerobic and anoxic conditions (both ranging from 2.57 to 3.58). The CAT and
405 POD antioxidant enzymes of the SRB1 consortium possessed low activities under all
406 exposure conditions, consistent with an earlier report (Okabe et al., 2023). The SOD activities
407 of aerobic and facultative bacteria were between 10.9 and 49.7, and the normal SOD activity
408 of aero-tolerant anaerobic bacteria was from 0.44 to 19.6 (Tally et al., 1977; Rolfe et al.,
409 1978). Therefore, the high SOD activity level of the SRB1 consortium under aerobic
410 conditions can further explain the survival of SRB in an oxygen-containing environment.

411 3.5 Possible survival mechanisms and environmental implications

412 A model of As^{3+} immobilization and survival strategy by the SRB1 consortium under
413 aerobic conditions is proposed in Fig. 7. Under aerobic conditions, the SRB1 consortium
414 retained the ability to reduce SO_4^{2-} and immobilize As^{3+} into arsenic sulfides (As_4S_4 and AsS),
415 which was consistent with our previous findings of products under anaerobic conditions (Li

416 et al., 2022b). However, redissolution of arsenic likely occurs at a later stage under aerobic
417 conditions. Additionally, the abundance of *Desulfovibrio* clearly decreased under aerobic
418 conditions, whereas the aerobic *Pseudomonas* was significantly enriched. Bacterial
419 interaction analysis demonstrates a positive correlation between *Desulfovibrio* and
420 *Pseudomonas*. The enriched strains of *Pseudomonas* likely consume more oxygen, which
421 would create a niche for the *Desulfovibrio* in the SRB1 consortium (Chen et al., 2023). It
422 seems reasonable that the SRB1 consortium produces additional EPS (PN) and exhibited high
423 antioxidative enzyme activity such as SOD to reduce ROS toxicity and survive in the
424 presence of excess oxygen.

425 Therefore, the survival of SRB in oxygen-containing environments may be related to the
426 contribution of coexisting (mutualistic-symbiotic) bacteria providing a niche for
427 *Desulfovibrio* by consuming oxygen in the environment and increasing their oxygen
428 tolerance levels, as well as enabling the SRB to generate EPS and SOD as additional
429 adaptation strategies. The complex mechanisms involved in the contribution of these
430 co-existing bacteria to engender *Desulfovibrio* oxygen resistance under aerobic conditions
431 were not confirmed here using pure strains. Future studies are planned to use metagenomics
432 to uncover the underlying mechanisms of oxidative stress of the SRB1 consortium in an
433 oxygen-containing water environment, as well as to identify the effects of oxygen on SRB1
434 incubated in actual environmental media (soil and water samples). It is anticipated that these
435 studies will stimulate the interest of researchers and environmental engineers to utilize SRB
436 as a remediation tool to treat HM-contaminated wastewater or tailings. The present study
437 furthers the awareness of traditional anaerobic SRB and provides a deeper understanding of

438 the biogeochemical behavior of SRB for future studies in the laboratory or field.

439 **4. Conclusion**

440 SRBs are generally regarded as strict anaerobic bacteria, which play a potential role in
441 the bioremediation of nonferrous metal-contaminated environments, but little is known about
442 the oxygen tolerance mechanism of SRB and the effect of oxygen on the metalliferous
443 immobilization by SRB. In the present study, the immobilization mechanism of the SRB1
444 consortium on As^{3+} under anaerobic and aerobic conditions was compared, as well as the
445 survival strategy of SRB1 under oxygen-containing conditions was illustrated. The studied
446 enriched sulfate-reducing consortium (SRB1) can generate additional EPS and SOD which
447 were rich in functionalities such as Fe-O, S=O, C=O, and -OH under aerobic conditions to
448 resist As^{3+} stress and oxygen toxicity. Such functional groups could potentially scavenge
449 oxygen and also act as binding sites for As^{3+} leading to its immobilization under aerobic
450 conditions. In contrast, this consortium showed similar As^{3+} immobilization activities under
451 both conditions, such as the formation of As^{3+} bioprecipitates under both conditions, mainly
452 arsenic minerals (AsS and As_4S_4) identified by XRD and XPS analysis. The anaerobic
453 *Desulfovibrio* was positively correlated with aerobic *Pseudomonas* suggesting the potential
454 symbiotic strategy to adapt to As^{3+} stress. We posit that the survival strategy of *Desulfovibrio*
455 in the SRB1 consortium under aerobic conditions is attributed to co-existing bacteria that
456 consume oxygen, providing a niche for *Desulfovibrio* and thus improving its tolerance to
457 oxygen. On the other hand, another adaptation strategy of *Desulfovibrio* to the aerobic
458 environment is the production of additional EPS and SOD. To our knowledge, this is the first
459 report on the immobilization and survival strategy of SRB for As^{3+} under aerobic conditions.

460 This study presents new insights into the oxygen tolerance and detoxification mechanism of
461 SRB and provides a basis for future engineering applications of SRB as a remediation tool.

462

463 **Acknowledgments**

464 This work has been supported partly by grants received from the Major National R & D
465 Projects from the Chinese Ministry of Science and Technology (2019YFC1803500,
466 2021YFE0106600), the National Science Foundation of China (42230716), the 111 Project
467 (B21017) and the 1000-Talents Plan Project (WQ2017110423). We thank Dr. Jihai Gu
468 (Hebei University) and Professor Jalal Hawari (Ecole Polytechnique de Montréal) for their
469 comments and review of an earlier version of this manuscript.

470

471 **Author contributions**

472 **Miaomiao Li and Yating Wang:** Conceptualization, Methodology, Resources, Formal
473 analysis, Writing - original draft, Writing – review & editing. **Jun Yao:** Writing – review &
474 editing, Funding acquisition. **Geoffrey Sunahara and Bang Liu:** Conceptualization, Data
475 Curation, Visualization, Writing – review & editing. **Jianli Liu, Houquan Liu, Bo Ma, Hao
476 Li, Wancheng Pang and Ying Cao:** Writing – review & editing.

477

478

479 **References**

- 480 Bao, Y.P., Jin, X.H., Guo, C.L., Lu, G.N., Dang, Z., 2020. Sulfate-reducing bacterial
481 community shifts in response to acid mine drainage in the sediment of the Hengshi
482 watershed, South China. *Environ. Sci. Pollut. Res.* 28(3), 2822-2834. doi:
483 10.1007/s11356-020-10248-7
- 484 Barakan, S., Aghazadeh, V., Samiee Beyragh, A., Mohammadi, S., 2019. Thermodynamic,
485 kinetic and equilibrium isotherm studies of As(V) adsorption by Fe(III)-impregnated
486 bentonite. *Environ. Dev. Sustain.* 22(6), 5273-5295. doi:
487 10.1007/s10668-019-00424-2
- 488 Chen, M.J., Zhang, Z.F., Hu, X.J., Tian, J.P., Lu, Z.Y., Wang, J.S., Wan, R.D., Zhou, X., Zhou,
489 X.J., Shen, P.L., Liu, D.W., 2022. Oxidation mechanism of arsenopyrite under
490 alkaline conditions: Experimental and theoretical analyses. *J. Clean. Prod.* 358. doi:
491 10.1016/j.jclepro.2022.131987
- 492 Chen, W.Y., Wu, J.H., Wang, B.N., 2023. Intermittent oxygen supply facilitates codegradation
493 of trichloroethene and toluene by anaerobic consortia. *Environ. Sci. Technol.* 57(28),
494 10252-10262. doi: 10.1021/acs.est.3c02481
- 495 Chen, Y.W., Zhang, Z.H., 2019. Oxygen tolerance of sulfate reducing bacteria in fresh and
496 coastal sea waters under enrichment culture conditions. *Geological Journal of China*
497 *Universities.* 25(5), 705-713. doi: 10.16108/j.issn1006-7493.2019025
- 498 Chun, S.J., Kim, Y.J., Cui, Y.S., Nam, K.H., 2021. Ecological network analysis reveals
499 distinctive microbial modules associated with heavy metal contamination of
500 abandoned mine soils in Korea. *Environ. Pollut.* 289, 117851. doi:
501 10.1016/j.envpol.2021.117851
- 502 Cypionka, H., Widdel, F., Pfennig, N., 1985. Survival of sulfate-reducing bacteria after
503 oxygen stress, and growth in sulfate-free oxygen-sulfide gradients. *FEMS Microbiol.*
504 *Lett.* 31(1), 39-45. doi: 10.1111/j.1574-6968.1985.tb01129.x
- 505 Dalsgaard, T., Stewart, F.J., Thamdrup, B., De Brabandere, L., Revsbech, N.P., Ulloa, O.,
506 Canfield, D.E., DeLong, E.F., 2014. Oxygen at nanomolar levels reversibly
507 suppresses process rates and gene expression in anammox and denitrification in the

508 oxygen minimum zone off northern Chile. *Mbio.* 5(6). doi: 10.1128/mBio.01966-14
509 de Matos, L.P., Costa, P.F., Moreira, M., Gomes, P.C.S., de Queiroz Silva, S., Gurgel, L.V.A.,
510 Teixeira, M.C., 2018. Simultaneous removal of sulfate and arsenic using immobilized
511 non-traditional SRB mixed culture and alternative low-cost carbon sources. *Chem.*
512 *Eng. J.* 334, 1630-1641. doi: 10.1016/j.cej.2017.11.035
513 Dev, S., Galey, M., Chun, C.L., Novotny, C., Ghosh, T., Aggarwal, S., 2021. Enrichment of
514 psychrophilic and acidophilic sulfate-reducing bacterial consortia-a solution toward
515 acid mine drainage treatment in cold regions. *Environ Sci Process Impacts.* 23(12),
516 2007-2020. doi: 10.1039/d1em00256b
517 Fei, X.F., Christakos, G., Xiao, R., Ren, Z.Q., Liu, Y., Lv, X.N., 2019. Improved heavy metal
518 mapping and pollution source apportionment in Shanghai City soils using auxiliary
519 information. *Sci. Total Environ.* 661, 168-177. doi: 10.1016/j.scitotenv.2019.01.149
520 Feng, S.S., Li, K.J., Huang, Z.Z., Tong, Y.J., Yang, H.L., 2019. Specific mechanism of
521 *Acidithiobacillus caldus* extracellular polymeric substances in the bioleaching of
522 copper-bearing sulfide ore. *Plos One.* 14(4). doi: 10.1371/journal.pone.0213945
523 Feng, X.N., Liu, Q.Y., Wang, S., Cen, L., Li, H.P., 2021. Arsenopyrite weathering in acid rain:
524 Arsenic transfer and environmental implications. *J. Hazard. Mater.* 420, 126612. doi:
525 10.1016/j.jhazmat.2021.126612
526 Fourçans, A., Ranchou-Peyruse, A., Caumette, P., Duran, R., 2007. Molecular analysis of the
527 spatio-temporal distribution of sulfate-reducing bacteria (SRB) in Camargue (France)
528 hypersaline microbial mat. *Microb. Ecol.* 56(1), 90-100. doi:
529 10.1007/s00248-007-9327-x
530 Fournier, M., Dermoun, Z., Durand, M.C., Dolla, A., 2004. A new function of the
531 *Desulfovibrio vulgaris* Hildenborough [Fe] hydrogenase in the protection against
532 oxidative stress. *J. Biol. Chem.* 279(3), 1787-1793. doi: 10.1074/jbc.M307965200
533 Giloteaux, L., Duran, R., Casiot, C., Bruneel, O., Elbaz-Poulichet, F., Goñi-Urriza, M., 2013.
534 Three-year survey of sulfate-reducing bacteria community structure in Carnoulès acid
535 mine drainage (France), highly contaminated by arsenic. *FEMS Microbiol. Ecol.*
536 83(3), 724-737. doi: 10.1111/1574-6941.12028
537 Gu, W.Z., Zheng, D.C., Li, D.P., Wei, C.C., Wang, X., Yang, Q.Z.M., Tian, C., Cui, M.Y.,

538 2021. Integrative effect of citrate on Cr(VI) and total Cr removal using a
539 sulfate-reducing bacteria consortium. *Chemosphere*. 279, 130437. doi:
540 10.1016/j.chemosphere.2021.130437

541 Hwang, S.K., Jho, E.H., 2018. Heavy metal and sulfate removal from sulfate-rich synthetic
542 mine drainages using sulfate reducing bacteria. *Sci. Total Environ*. 635, 1308-1316.
543 doi: 10.1016/j.scitotenv.2018.04.231

544 Jenney, F.E., Verhagen, M.F.J.M., Cui, X.Y., Adams, M.W.W., 1999. Anaerobic microbes:
545 Oxygen detoxification without superoxide dismutase. *Science*. 286, 306-309. doi:
546 10.1126/science.286.5438.30

547 Jia, T.P., Zhang, L., Zhao, Q., Peng, Y.Z., 2022. The effect of biofilm growth on the sulfur
548 oxidation pathway and the synergy of microorganisms in desulfurization reactors
549 under different pH conditions. *J. Hazard. Mater*. 432, 128638. doi:
550 10.1016/j.jhazmat.2022.128638

551 Jin, Q.S., Kirk, M.F., 2018. pH as a primary control in environmental microbiology: 1.
552 Thermodynamic perspective. *Front. Environ. Sci*. 6. doi: 10.3389/fenvs.2018.00021

553 Kieu, H.T.Q., Müller, E., Horn, H., 2011. Heavy metal removal in anaerobic semi-continuous
554 stirred tank reactors by a consortium of sulfate-reducing bacteria. *Water Res*. 45(13),
555 3863-3870. doi: 10.1016/j.watres.2011.04.043

556 Li, H., Yao, J., Min, N., Chen, Z.H., Li, M.M., Pang, W.C., Liu, B., Cao, Y., Men, D.Y.,
557 Duran, R., 2022a. Comprehensive evaluation of metal(loid)s pollution risk and
558 microbial activity characteristics in non-ferrous metal smelting contaminated site. *J.*
559 *Clean. Prod*. 344. doi: 10.1016/j.jclepro.2022.130999

560 Li, M.M., Yao, J., Sunahara, G., Duran, R., Liu, B., Cao, Y., Li, H., Pang, W.C., Liu, H.Q.,
561 Jiang, S., Zhu, J.J., Zhang, Q.H., 2023. Assembly processes of bacterial and fungal
562 communities in metal(loid)s smelter soil. *J. Hazard. Mater*. 451, 131153. doi:
563 10.1016/j.jhazmat.2023.131153

564 Li, M.M., Yao, J., Sunahara, G., Hawari, J., Duran, R., Liu, J.L., Liu, B., Cao, Y., Pang, W.C.,
565 Li, H., Li, Y.Q., Ruan, Z.Y., 2022b. Novel microbial consortia facilitate metalliferous
566 immobilization in non-ferrous metal(loid)s contaminated smelter soil: Efficiency and
567 mechanisms. *Environ. Pollut*. 313, 120042. doi: 10.1016/j.envpol.2022.120042

568 Li, P.Z., Lin, C.Y., Cheng, H.G., Duan, X.L., Lei, K., 2015. Contamination and health risks of
569 soil heavy metals around a lead/zinc smelter in southwestern China. *Ecotoxicol.*
570 *Environ. Saf.* 113, 391-9. doi: 10.1016/j.ecoenv.2014.12.025

571 Li, Y., Dong, C.L., Li, Y., Nie, W.Q., Wang, M.W., Sun, C., Liang, L.F., Zhao, Z.Q., Zhang,
572 Y.B., 2022c. Independent of direct interspecies electron transfer: Magnetite-mediated
573 sulphur cycle for anaerobic degradation of benzoate under low-concentration sulphate
574 conditions. *J. Hazard. Mater.* 423. doi: 10.1016/j.jhazmat.2021.127051

575 Liu, B.L., Ai, S.W., Zhang, W.Y., Huang, D.J., Zhang, Y.M., 2017. Assessment of the
576 bioavailability, bioaccessibility and transfer of heavy metals in the soil-grain-human
577 systems near a mining and smelting area in NW China. *Sci. Total Environ.* 609,
578 822-829. doi: 10.1016/j.scitotenv.2017.07.215

579 Liu, F.J., Zhang, G.P., Liu, S.R., Fu, Z.P., Chen, J.J., Ma, C., 2018. Bioremoval of arsenic and
580 antimony from wastewater by a mixed culture of sulfate-reducing bacteria using
581 lactate and ethanol as carbon sources. *Int. Biodeter. Biodegr.* 126, 152-159. doi:
582 10.1016/j.ibiod.2017.10.011

583 Liu, Y., Serrano, A., Wyman, V., Marcellin, E., Southam, G., Vaughan, J., Villa-Gomez, D.,
584 2021. Nickel complexation as an innovative approach for nickel-cobalt selective
585 recovery using sulfate-reducing bacteria. *J. Hazard. Mater.* 402. doi:
586 10.1016/j.jhazmat.2020.123506

587 Lv, Y., Zhu, X.Y., Zhang, M.J., Liu, X.Y., Wang, J.L., 2022. In-situ bioremediation of
588 multiple heavy metals contaminated farmland soil by sulfate-reducing bacteria. *Pol. J.*
589 *Environ. Stud.* 31(2), 1747-1755. doi: 10.15244/pjoes/141326

590 More, T.T., Yadav, J.S.S., Yan, S., Tyagi, R.D., Surampalli, R.Y., 2014. Extracellular
591 polymeric substances of bacteria and their potential environmental applications. *J.*
592 *Environ. Manage.* 144, 1-25. doi: 10.1016/j.jenvman.2014.05.010

593 Morris, J.G. 1975. The physiology of obligate anaerobiosis. *Adv. Microb. Physiol.* 169-246.
594 doi: 10.1016/s0065-2911(08)60282-9

595 Nagar, S., Talwar, C., Motelica-Heino, M., Richnow, H.H., Shakarad, M., Lal, R., Negi, R.K.,
596 2022. Microbial ecology of sulfur biogeochemical cycling at a mesothermal hot
597 spring atop northern Himalayas, India. *Front. Microbiol.* 13. doi:

598 10.3389/fmicb.2022.848010

599 Nguyen, D., Wu, Z.Y., Shrestha, S., Lee, P.H., Raskin, L., Khanal, S.K., 2019. Intermittent
600 micro-aeration: New strategy to control volatile fatty acid accumulation in high
601 organic loading anaerobic digestion. *Water Res.* 166. doi:
602 10.1016/j.watres.2019.115080

603 Okabe, S., Ye, S.Y., Lan, X., Nukada, K., Zhang, H.Z., Kobayashi, K., Oshiki, M., 2023.
604 Oxygen tolerance and detoxification mechanisms of highly enriched planktonic
605 anaerobic ammonium-oxidizing (anammox) bacteria. *ISME Commun.* 3(1). doi:
606 10.1038/s43705-023-00251-7

607 Oshiki, M., Satoh, H., Okabe, S., 2016. Ecology and physiology of anaerobic ammonium
608 oxidizing bacteria. *Environ. Microbiol.* 18(9), 2784-2796. doi:
609 10.1111/1462-2920.13134

610 Ramel, F., Amrani, A., Pieulle, L., Lamrabet, O., Voordouw, G., Seddiki, N., Brèthes, D.,
611 Company, M., Dolla, A., Brasseur, G., 2013. Membrane-bound oxygen reductases of
612 the anaerobic sulfate-reducing *Desulfovibrio vulgaris* Hildenborough: roles in oxygen
613 defence and electron link with periplasmic hydrogen oxidation. *Microbiology.*
614 159(Pt_12), 2663-2673. doi: 10.1099/mic.0.071282-0

615 Ramel, F., Brasseur, G., Pieulle, L., Valette, O., Hirschler-Réa, A., Fardeau, M.L., Dolla, A.,
616 2015. Growth of the obligate anaerobe *Desulfovibrio vulgaris* Hildenborough under
617 continuous low oxygen concentration sparging: Impact of the membrane-bound
618 oxygen reductases. *Plos One.* 10(4). doi: 10.1371/journal.pone.0123455

619 Ran, H.Z., Guo, Z.H., Yi, L.W., Xiao, X.Y., Zhang, L., Hu, Z.H., Li, C.Z., Zhang, Y.X., 2021.
620 Pollution characteristics and source identification of soil metal(loid)s at an abandoned
621 arsenic-containing mine, China. *J. Hazard. Mater.* 413. doi:
622 10.1016/j.jhazmat.2021.125382

623 Ravenschlag, K., Sahn, K., Knoblauch, C., Jørgensen, B.B., Amann, R., 2000. Community
624 structure, cellular rRNA content, and activity of sulfate-reducing bacteria in marine
625 arctic sediments. *Appl. Environ. Microbiol.* 66(8), 3592-3602. doi:
626 10.1128/AEM.66.8.3592-3602.2000

627 Risatti, J.B., Capman, W.C., Stahl, D.A., 1994. Community structure of a microbial mat: the

628 phylogenetic dimension. Proc. Natl. Acad. Sci. USA. 91(21), 10173-10177. doi:
629 10.1073/pnas.91.21.10173

630 Rogers, K.L., Carreres-Calabuig, J.A., Gorokhova, E., Posth, N.R., 2020. Micro-by-micro
631 interactions: How microorganisms influence the fate of marine microplastics. Limnol.
632 Oceanogr. 5(1), 18-36. doi: 10.1002/lol2.10136

633 Rolfe, R.D., Hentges, D.J., Campbell, B.J., Barrett, J.T., 1978. Factors related to the oxygen
634 tolerance of anaerobic bacteria. Appl. Environ. Microbiol. 36, 306-313. doi:
635 10.1128/aem.36.2.306-313.1978

636 Shi, J.X., Zhang, B.G., Cheng, Y.T., Peng, K.J., 2020. Microbial vanadate reduction coupled
637 to co-metabolic phenanthrene biodegradation in groundwater. Water Res. 186, 116354.
638 doi: 10.1016/j.watres.2020.116354

639 Si, S.C., Ke, Y.X., Xue, B.Q., Zhang, Z.Y., Zhu, X.L., 2023. Immobilized sulfate reducing
640 bacteria (SRB) enhanced passivation performance of biochar for Zn. Sci. Total
641 Environ. 892. doi: 10.1016/j.scitotenv.2023.164556

642 Sigalevich, P., Baev, M.V., Teske, A., Cohen, Y., 2000. Sulfate reduction and possible aerobic
643 metabolism of the sulfate-reducing bacterium *Desulfovibrio oxyclinae* in a chemostat
644 coculture with *Marinobacter* sp. strain MB under exposure to increasing oxygen
645 concentrations. Appl. Environ. Microbiol. 66(11), 5013 - 5018. doi:
646 10.1128/AEM.66.11.5013-5018.2000

647 Sun, W.M., Xiao, E.Z., Xiao, T.F., Krumins, V., Wang, Q., Häggblom, M., Dong, Y.R., Tang,
648 S., Hu, M., Li, B.Q., Xia, B.Q., Liu, W., 2017. Response of soil microbial
649 communities to elevated antimony and arsenic contamination indicates the
650 relationship between the innate microbiota and contaminant fractions. Environ. Sci.
651 Technol. 51(16), 9165-9175. doi: 10.1021/acs.est.7b00294

652 Tally, F.P., Goldin, B.R., Jacobus, N.V., Gorbach, S.L., 1977. Superoxide dismutase in
653 anaerobic bacteria of clinical significance. Infect. Immun. 16(1), 20-25. doi:
654 10.1128/iai.16.1.20-25.1977

655 Vita, N., Hatchikian, E.C., Nouailler, M., Dolla, A., Pieulle, L., 2008. Disulfide
656 bond-dependent mechanism of protection against oxidative stress in
657 pyruvate-ferredoxin oxidoreductase of anaerobic *Desulfovibrio* bacteria. Biochemistry.

658 47(3), 957–964. doi: 10.1021/bi7014713

659 Wang, J., Li, Q., Li, M.M., Chen, T.H., Zhou, Y.F., Yue, Z.B., 2014. Competitive adsorption
660 of heavy metal by extracellular polymeric substances (EPS) extracted from sulfate
661 reducing bacteria. *Bioresour. Technol.* 163, 374-376. doi:
662 10.1016/j.biortech.2014.04.073

663 Wang, Z.L., Zhang, B.G., He, C., Shi, J.X., Wu, M.X., Guo, J.H., 2021. Sulfur-based
664 mixotrophic vanadium (V) bio-reduction towards lower organic requirement and
665 sulfate accumulation. *Water Res.* 189, 116655. doi: 10.1016/j.watres.2020.116655

666 Wu, Z.T., Chen, Z.Y., Huang, W.H., Wei, Z.S., 2023. Flue gas arsenic trioxide removal from
667 sludge incineration by sulfate-reducing membrane biofilm reactor. *Fuel.* 346. doi:
668 10.1016/j.fuel.2023.128295

669 Xiao, R., Guo, D., Ali, A., Mi, S.S., Liu, T., Ren, C.Y., Li, R.H., Zhang, Z.Q., 2019.
670 Accumulation, ecological-health risks assessment, and source apportionment of heavy
671 metals in paddy soils: A case study in Hanzhong, Shaanxi, China. *Environ. Pollut.* 248,
672 349-357. doi: 10.1016/j.envpol.2019.02.045

673 Xu, C.F., Su, X., Wang, J.H., Zhang, F.Z., Shen, G.N., Yuan, Y., Yan, L., Tang, H.Z., Song,
674 F.Q., Wang, W.D., 2021a. Characteristics and functional bacteria in a microbial
675 consortium for rice straw lignin-degrading. *Bioresour. Technol.* 331, 125066. doi:
676 10.1016/j.biortech.2021.125066

677 Xu, D.M., Fu, R.B., 2022. Mechanistic insight into the release behavior of arsenic (As) based
678 on its geochemical fractions in the contaminated soils around lead/zinc (Pb/Zn)
679 smelters. *J. Clean. Prod.* 363. doi: 10.1016/j.jclepro.2022.132348

680 Xu, D.M., Fu, R.B., Liu, H.Q., Guo, X.P., 2021b. Current knowledge from heavy metal
681 pollution in Chinese smelter contaminated soils, health risk implications and
682 associated remediation progress in recent decades: A critical review. *J. Clean. Prod.*
683 286. doi: 10.1016/j.jclepro.2020.124989

684 Yan, J., Ye, W.Z., Liang, X.S., Wang, S.J., Xie, J.H., Zhong, K.Q., Bao, M., Yang, J.B., Wen,
685 H.J., Li, S.G., Chen, Y.H., Gu, J.D., Zhang, H.G., 2020. Enhanced reduction of sulfate
686 and chromium under sulfate-reducing condition by synergism between extracellular
687 polymeric substances and graphene oxide. *Environ. Res.* 183. doi:

688 10.1016/j.envres.2020.109157
689 Yan, X., Guan, D.X., Li, J., Song, Y.X., Tao, H., Zhang, X.M., Ma, M., Ji, J.F., Zhao, W.C.,
690 2023. Fate of Cd during mineral transformation by sulfate-reducing bacteria in
691 clay-size fractions from soils with high geochemical background. *J. Hazard. Mater.*
692 459. doi: 10.1016/j.jhazmat.2023.132213
693 Yue, X., Yu, G.P., Lu, Y.Q., Liu, Z.H., Li, Q.H., Tang, J.L., Liu, J., 2018. Effect of dissolved
694 oxygen on nitrogen removal and the microbial community of the completely
695 autotrophic nitrogen removal over nitrite process in a submerged aerated biological
696 filter. *Bioresour. Technol.* 254, 67-74. doi: 10.1016/j.biortech.2018.01.044
697 Yun, S.W., Baveye, P.C., Kim, D.H., Kang, D.H., Lee, S.Y., Kong, M.J., Park, C.G., Kim,
698 H.D., Son, J., Yu, C., 2018. Analysis of metal(loid)s contamination and their
699 continuous input in soils around a zinc smelter: development of methodology and a
700 case study in south Korea. *Environ. Pollut.* 238, 140-149. doi:
701 10.1016/j.envpol.2018.03.020
702 Zampieri, B.D.B., Nogueira, E.W., de Oliveira, A.J.F.C., Sanchez-Andrea, I., Brucha, G.,
703 2021. Effects of metals on activity and community of sulfate-reducing bacterial
704 enrichments and the discovery of a new heavy metal-resistant SRB from Santos Port
705 sediment (Sao Paulo, Brazil). *Environ. Sci. Pollut. Res.* doi:
706 10.1007/s11356-021-15418-9
707 Zhang, B.G., Cheng, Y.T., Shi, J.X., Xing, X., Zhu, Y.L., Xu, N., Xia, J.X., Borthwick, A.G.L.,
708 2019. Insights into interactions between vanadium (V) bio-reduction and
709 pentachlorophenol dechlorination in synthetic groundwater. *Chem. Eng. J.* 375. doi:
710 10.1016/j.cej.2019.121965
711 Zhang, H.W., Zhang, F., Song, J., Tan, M.L., Kung, H.T., Johnson, V.C., 2021. Pollutant
712 source, ecological and human health risks assessment of heavy metals in soils from
713 coal mining areas in Xinjiang, China. *Environ. Res.* 202. doi:
714 10.1016/j.envres.2021.111702
715 Zhao, M.M., Zheng, G.G., Kang, X.Y., Zhang, X.Y., Guo, J.M., Zhang, M.X., Zhang, J.W.,
716 Chen, Y.P., Xue, L.G., 2023. Arsenic pollution remediation mechanism and
717 preliminary application of arsenic-oxidizing bacteria isolated from industrial

718 wastewater. Environ. Pollut. 324. doi: 10.1016/j.envpol.2023.121384
719 Zhou, C., Vannela, R., Hayes, K.F., Rittmann, B.E., 2014. Effect of growth conditions on
720 microbial activity and iron-sulfide production by *Desulfovibrio vulgaris*. J. Hazard.
721 Mater. 272, 28-35. doi: 10.1016/j.jhazmat.2014.02.046
722 Zhou, J.M., Xing, J.M., 2021. Haloalkaliphilic denitrifiers-dependent sulfate-reducing
723 bacteria thrive in nitrate-enriched environments. Water Res. 201. doi:
724 10.1016/j.watres.2021.117354
725
726

727 **Figure captions**

728 **Fig. 1.** Time course of pH and ORP (A), OD₆₀₀, and total As (B), and SO₄²⁻ and S²⁻ concentrations
729 (C) during 7 d of the As³⁺ immobilization of SRB1 consortium under anaerobic, anoxic, and
730 aerobic conditions. Data are expressed as mean ± SD (n = 3).

731 **Fig. 2.** Scanning electron microscope images of metal precipitates formed during a 7-d
732 biosynthesis process by SRB1 consortium under anaerobic (left column), anoxic (middle
733 column), and aerobic (right column) conditions.

734 **Fig. 3.** X-ray diffraction patterns of metal precipitates formed during a 7-d biosynthesis process by
735 SRB1 under anaerobic, anoxic, and aerobic conditions.

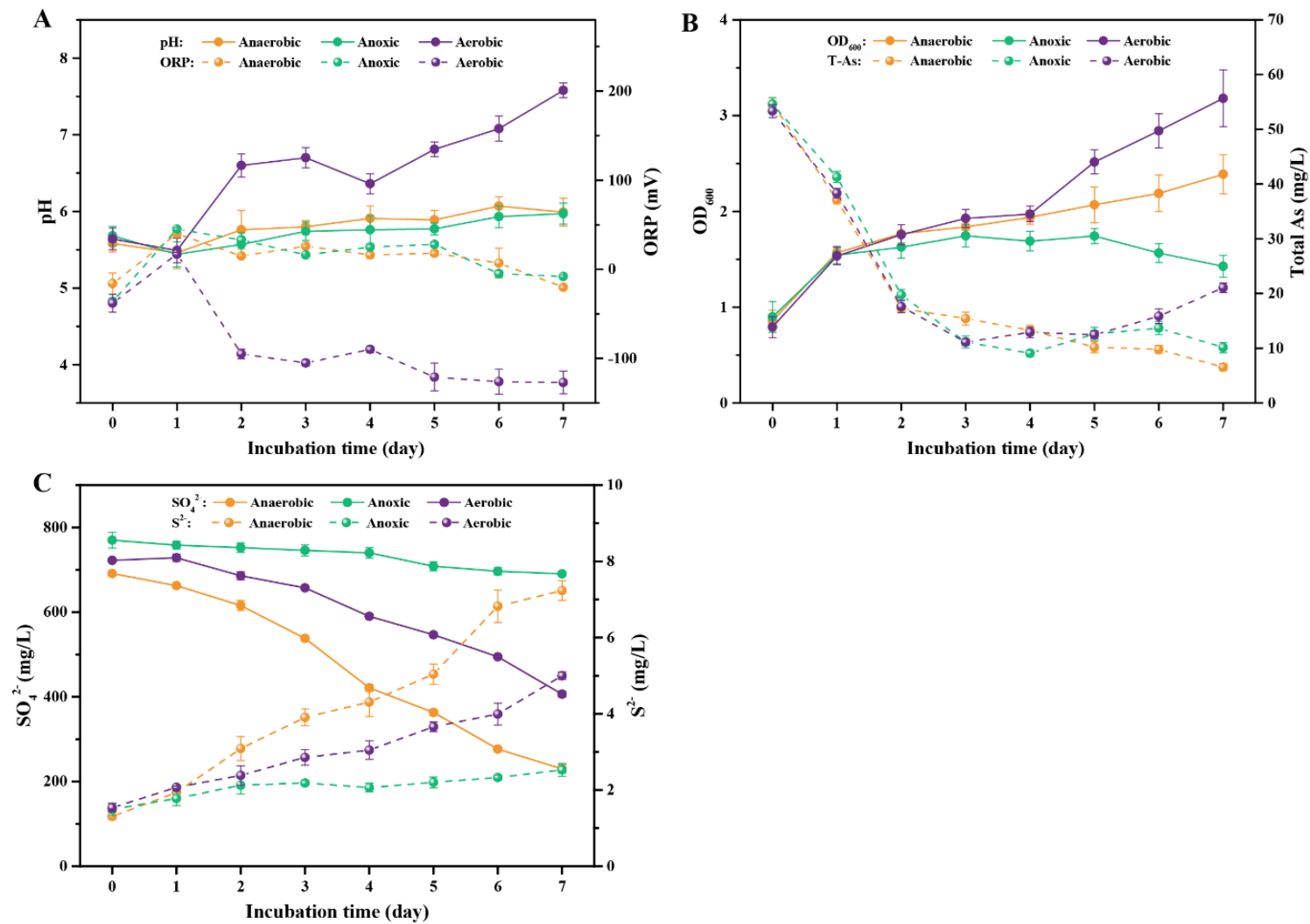
736 **Fig. 4.** XPS spectra of (A-C) As, (D-F) S, and (G-I) Fe species during 7 d of the As³⁺
737 immobilization of SRB1 consortium under anaerobic (panels A, D, and G), anoxic (B, E,
738 and H), and aerobic (C, F, and I) conditions.

739 **Fig. 5.** The compositions (A) and top 15 abundant genera (B) of the bacterial community of the
740 SRB1 consortium under anaerobic, anoxic, and aerobic conditions. Treatment group letters:
741 CK represents the initial inoculum, A, B, and C represent the anaerobic, anoxic, and aerobic
742 conditions, respectively. Different lowercase letters in the boxplots indicate significant
743 differences ($P < 0.05$) among different conditions.

744 **Fig. 6.** Co-occurrence patterns of SRB1 consortium. (A) At the phylum level, all the OTUs were
745 kept, (B) while at the genus level. Only those genera with the sum of relative abundances >
746 0.005 were kept and the OTUs were filtered that simultaneously appeared in five samples.
747 Edges are shown by strong correlations (Spearman $R > |0.7|$) and significant ($P < 0.05$). The
748 nodes were colored by phylum level. The thickness of the edges corresponds to the strength
749 of the correlation. Light pink lines indicate positive interactions and green lines indicate
750 negative interactions. (C) FTIR spectra of EPS at day 7, and (D) the mean extracellular
751 substance (EPS) content during 7 d of the As³⁺ immobilization of SRB1 consortium under
752 anaerobic, anoxic, and aerobic conditions. PS = polysaccharide, PN = extracellular protein,
753 and HS = humic-like substances.

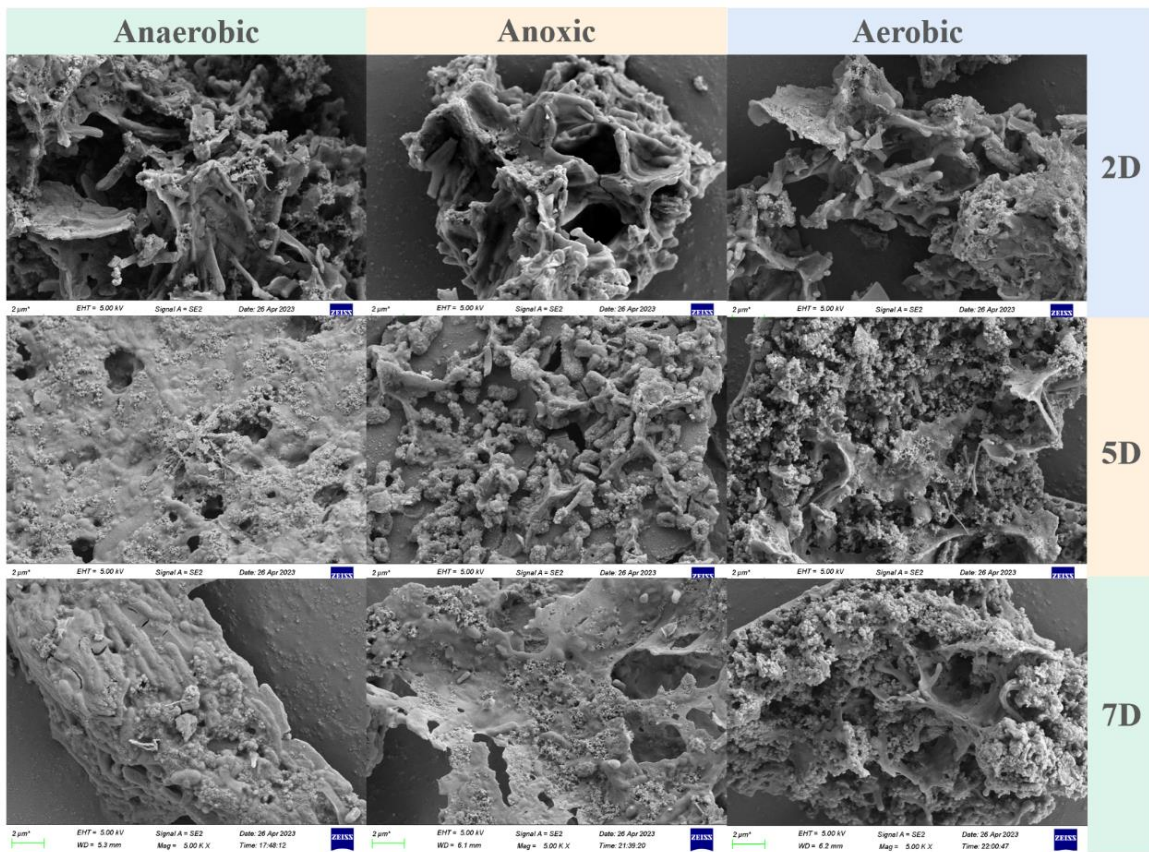
754 **Fig. 7.** A proposed model of As³⁺ immobilization and survival strategy by SRB1 consortium under
755 aerobic conditions.

756



757

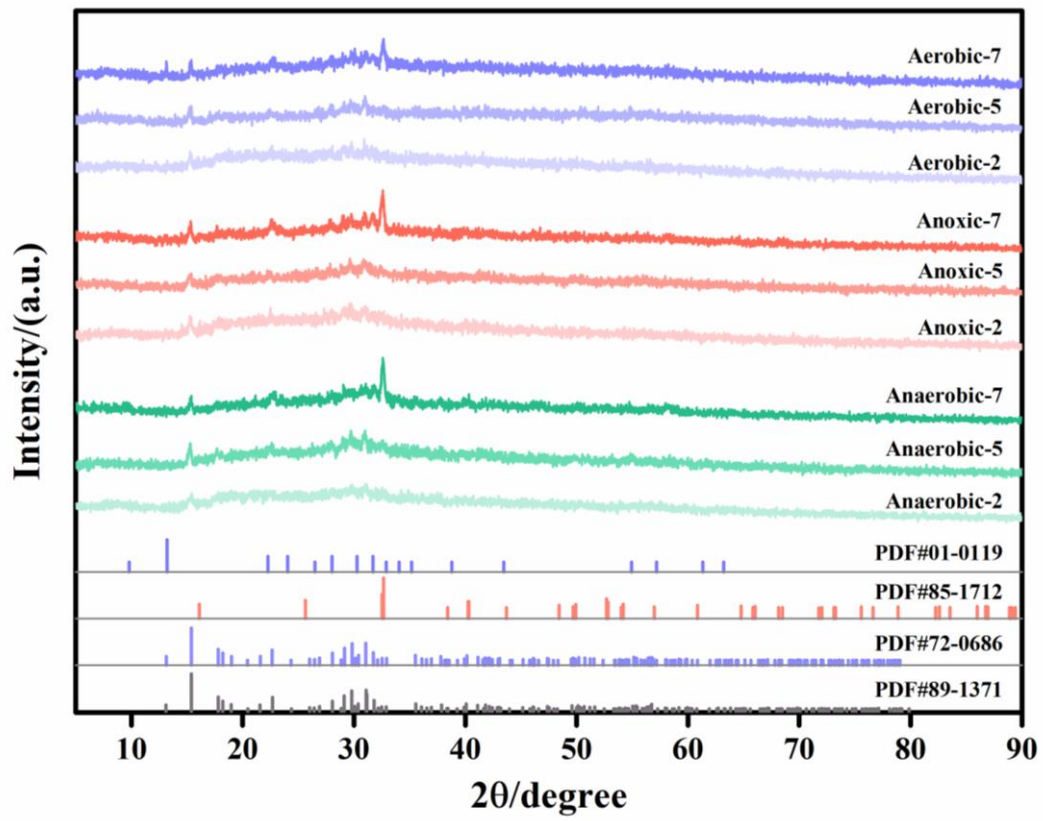
758 **Fig. 1.** Time course of pH and ORP (A), OD₆₀₀ and total As (B), and SO₄²⁻ and S²⁻ concentrations (C) during 7 d of the As³⁺ immobilization of
 759 SRB1 consortium under anaerobic, anoxic, and aerobic conditions. Data are expressed as mean ± SD (n = 3).



761

762 **Fig. 2.** Scanning electron microscope images of metal precipitates formed during a 7-d
 763 biosynthesis process by SRB1 consortium under anaerobic (left column), anoxic (middle
 764 column), and aerobic (right column) conditions.

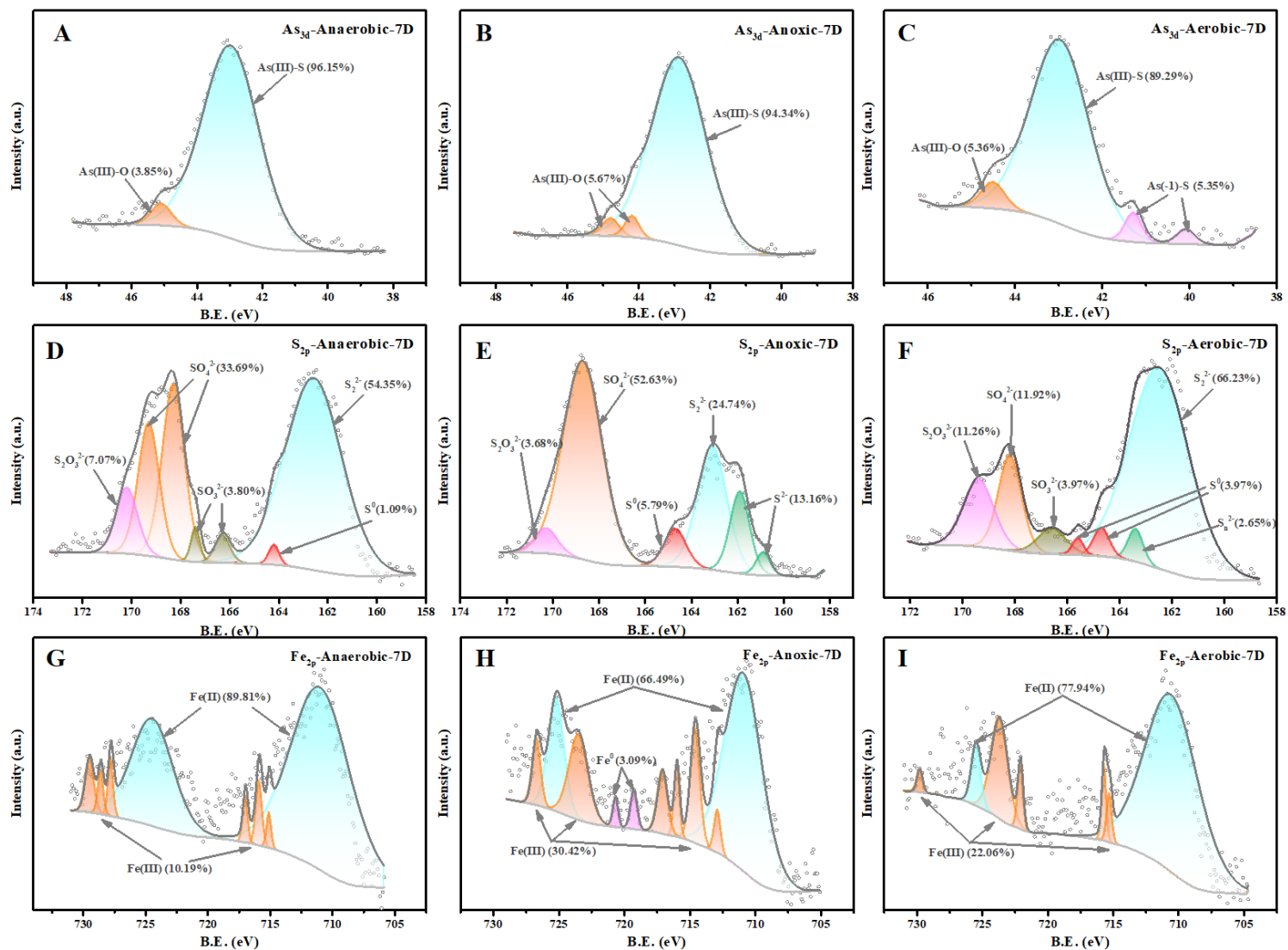
765



766

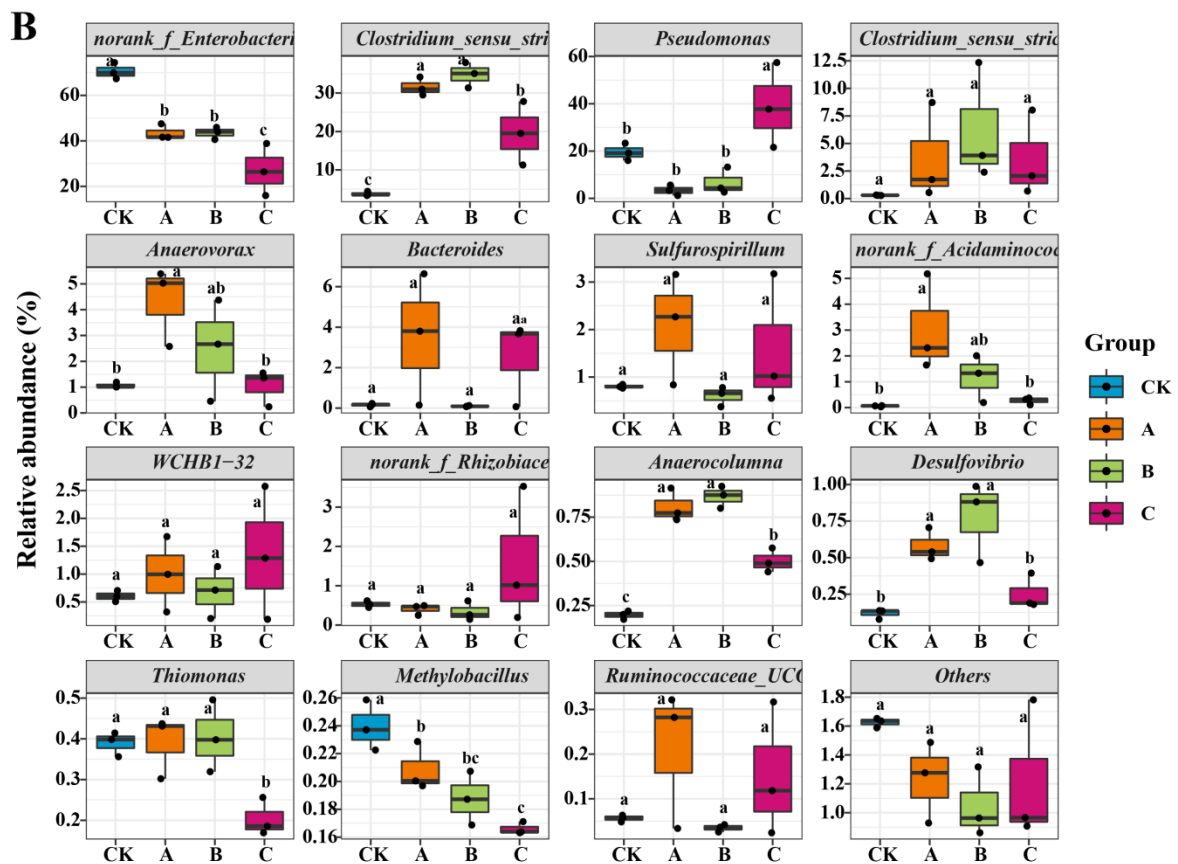
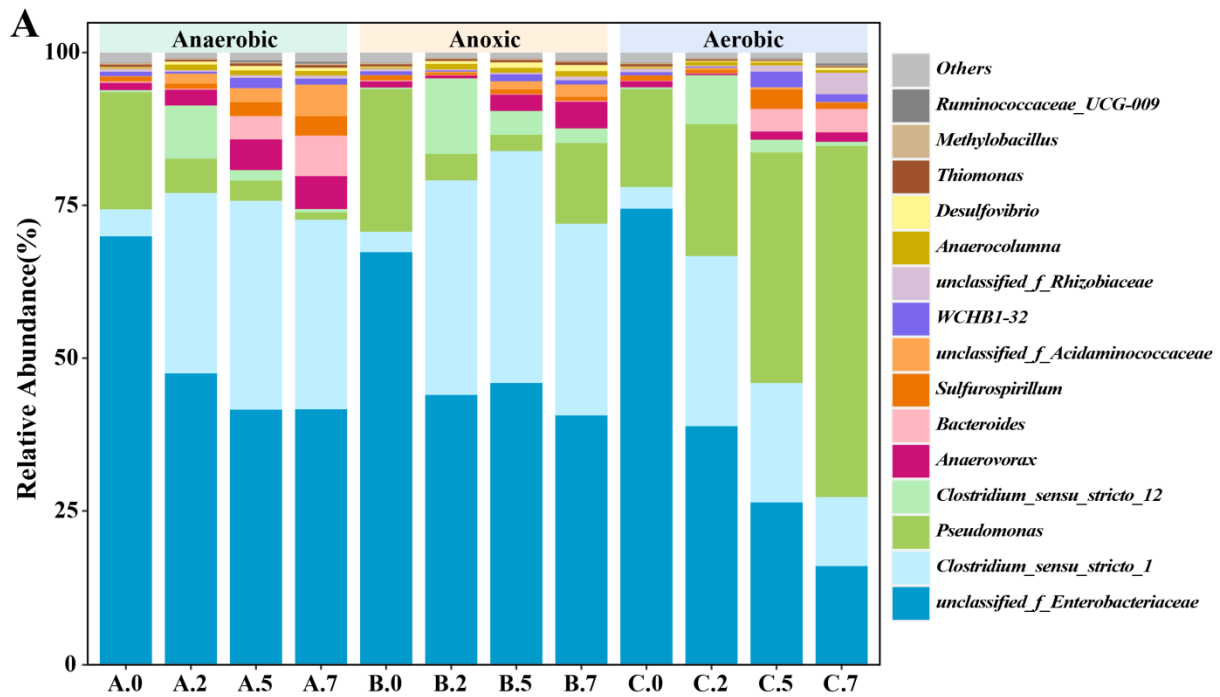
767 **Fig. 3.** X-ray diffraction patterns of metal precipitates formed during a 7-d biosynthesis
 768 process by SRB1 under anaerobic, anoxic, and aerobic conditions.

769



770

771 **Fig. 4.** XPS spectra of (A-C) As, (D-F) S, and (G-I) Fe species during 7 d of the As³⁺ immobilization of SRB1 consortium under anaerobic
 772 (panels A, D, and G), anoxic (B, E, and H), and aerobic (C, F, and I) conditions.



773

774

775

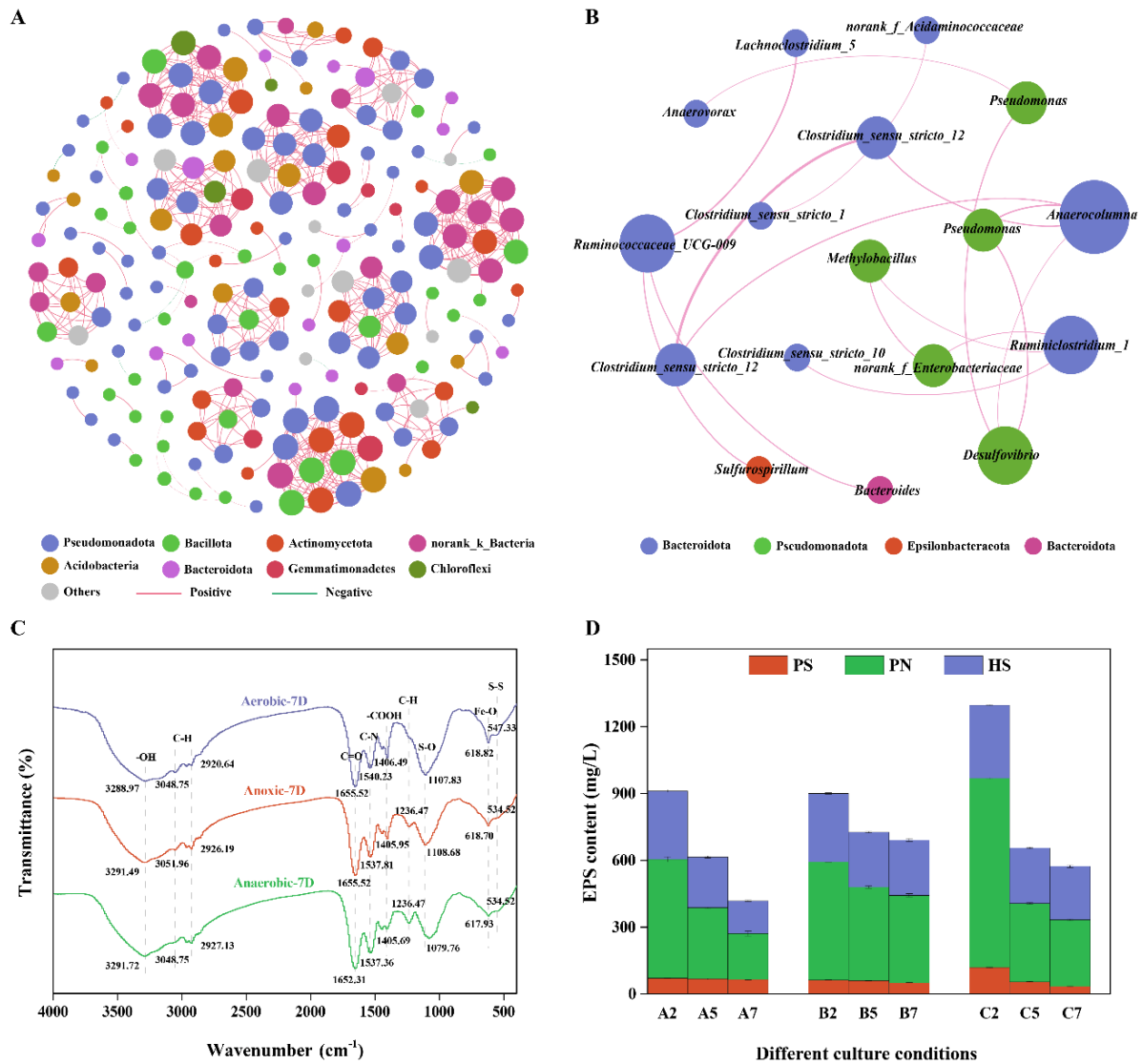
776

777

778

779

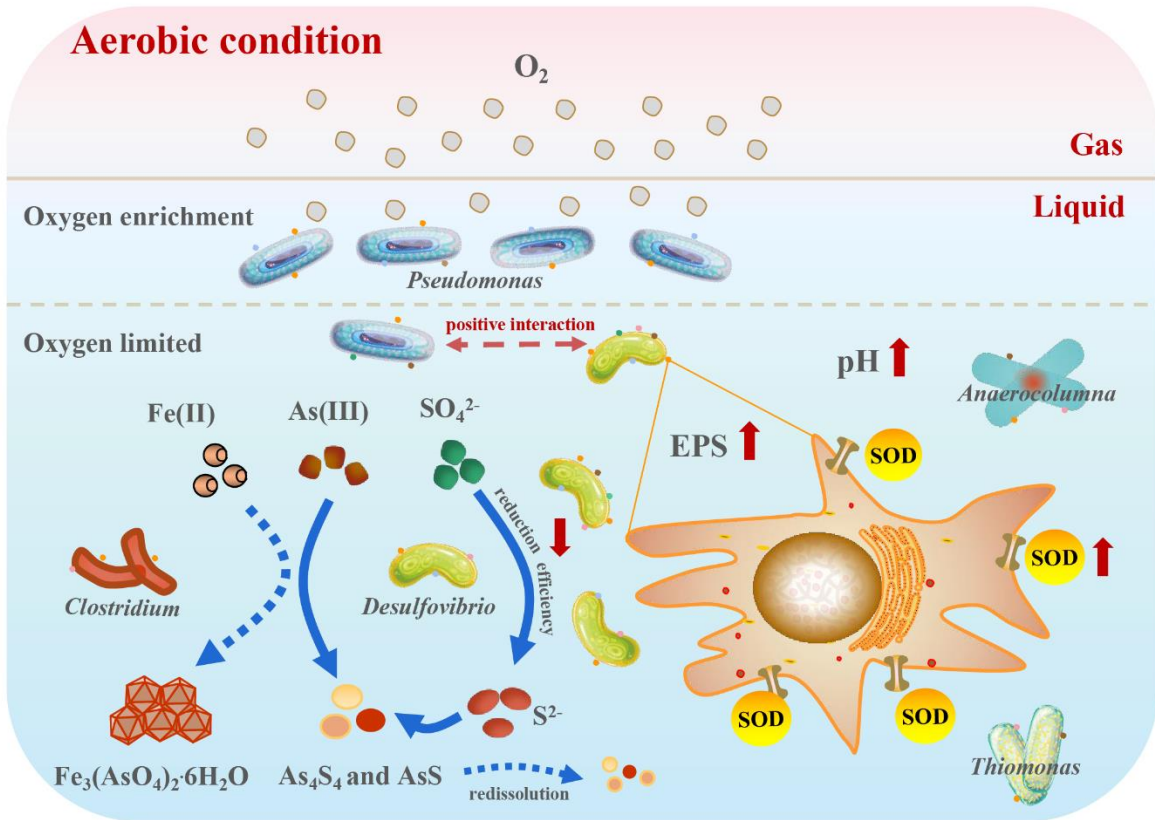
Fig. 5. The compositions (A) and top 15 abundant genera (B) of the bacterial community of the SRB1 consortium under anaerobic, anoxic, and aerobic conditions. Treatment group letters: CK represents the initial inoculum, A, B, and C represent the anaerobic, anoxic, and aerobic conditions, respectively. Different lowercase letters in the boxplots indicate significant differences ($P < 0.05$) among different conditions.



780

781 **Fig. 6.** Co-occurrence patterns of SRB1 consortium. (A) At the phylum level, all the OTUs
 782 were kept, (B) while at the genus level. Only those genera with the sum of relative
 783 abundances > 0.005 were kept and the OTUs were filtered that simultaneously appeared in
 784 five samples. Edges are shown by strong correlations (Spearman $R > |0.7|$) and significant (P
 785 < 0.05). The nodes were colored by phylum level. The thickness of the edges corresponds to
 786 the strength of the correlation. Light pink lines indicate positive interactions and green lines
 787 indicate negative interactions. (C) FTIR spectra of EPS at day 7, and (D) the mean
 788 extracellular substance (EPS) content during 7 d of the As^{3+} immobilization of SRB1
 789 consortium under anaerobic, anoxic, and aerobic conditions. PS = polysaccharide, PN =
 790 extracellular protein, and HS = humic-like substances.

791



792

793 **Fig. 7.** A proposed model of As³⁺ immobilization and survival strategy by SRB1 consortium

794 under aerobic conditions.